processes

MDPI

Article

Characteristics of Modified Complex of Red Mud and Phosphogypsum and Its Soil Substrate Utilization

Bin Liu [1], Zuyong Chen [2,*], Fang Liu [1] and Jian Zhu [1]

[1] College of Resource and Environmental Engineering, Guizhou University, Guiyang 550025, China; abin0705@163.com (B.L.); lfang6435@163.com (F.L.); zhujian2009@126.com (J.Z.)
[2] College of Agriculture, Guizhou University, Jiaxiu South Road, Huaxi District, Guiyang 550025, China
* Correspondence: zychen3@gzu.edu.cn

Abstract: The increasing generation of industrial solid wastes, such as red mud and phosphogypsum, poses significant environmental challenges due to their complex chemical compositions and low utilization rates. This study aims to develop an innovative composite material by combining RM and PG, modified with ferric chloride ($FeCl_3$) and sodium silicate (Na_2SiO_3), to address their environmental risks and enhance their potential for soil and ecological remediation. The modification mechanisms and immobilization of toxic ions were investigated through leaching behavior analysis and advanced microscopic techniques, including BET and XRD. Under the optimal ratio (RM:PG = 7:3), the composite material exhibited excellent performance, with stable pH (8.03), low electrical conductivity (4.89 mS/cm), and significantly reduced concentrations of phosphate (PO_4^{3-}: 0.36 mg/L) and fluoride ions (F^-: 1.34 mg/L), achieving an upgrade from industrial Class II to Class I slag. The modification process increased the specific surface area, optimized pore structure, and enhanced surface activity and structural stability. Pot experiments demonstrated that the modified composite supported normal plant growth, with leachate meeting Grade I wastewater discharge standards. This study not only provides a sustainable approach for the utilization of RM and PG, but also offers valuable insights into the development of eco-friendly materials for soil remediation and ecological restoration, benefiting both the scientific community and environmental management practices.

Keywords: red mud; phosphogypsum; modification complex; soil and ecological remediation

check for updates

Academic Editor: Guining Lu

Received: 7 March 2025
Revised: 22 March 2025
Accepted: 24 March 2025
Published: 25 March 2025

Citation: Liu, B.; Chen, Z.; Liu, F.; Zhu, J. Characteristics of Modified Complex of Red Mud and Phosphogypsum and Its Soil Substrate Utilization. *Processes* **2025**, *13*, 972. https://doi.org/10.3390/pr13040972

Copyright: © 2025 by the authors. Licensee MDPI, Basel, Switzerland. This article is an open access article distributed under the terms and conditions of the Creative Commons Attribution (CC BY) license (https://creativecommons.org/licenses/by/4.0/).

1. Introduction

Global industrialization has accelerated, leading to a significant increase in industrial waste generation. Among these wastes, red mud (RM) from the aluminum industry and phosphogypsum (PG) from the phosphate chemical industry are particularly challenging to manage due to their large production volumes and complex chemical compositions. Annual production of RM reaches 120 million tons, with its strong alkalinity (pH ~ 10–12) and potential toxic elements (e.g., heavy metals) limiting its utilization [1]. Similarly, PG, a primary byproduct of phosphate fertilizer production, has a global annual output exceeding 200 million tons. However, its high acidity (pH ~ 2–4) and high content of impurities such as phosphorus and fluoride make it environmentally risky industrial waste [2]. Improper disposal of these wastes not only occupies vast land areas, but also poses severe threats to water and soil quality, ultimately endangering ecological health [3].

The core objective of composite substrate preparation lies in achieving the synergistic utilization of red mud and phosphogypsum, two types of industrial solid waste. Red mud, as an alkaline industrial byproduct, not only possesses unique strong alkalinity (pH > 12),

excellent adsorption performance (specific surface area can reach 20–80 m^2/g) [4], and a well-developed hierarchical pore structure, but also contains significantly higher levels of potassium (1.5–3.0%) compared to ordinary soil [5]. Phosphogypsum, as an acidic industrial waste, typically has a pH below 3 but is rich in essential plant nutrients such as phosphorus (P_2O_5 content around 12–18%) [6], calcium (CaO content around 30–45%), and sulfur (SO_3 content around 40–50%), giving it potential for soil improvement [7]. By scientifically combining these two materials, the alkalinity of red mud can neutralize the acidity of phosphogypsum, simultaneously achieving chemical immobilization and physical encapsulation of heavy metal ions [8,9]. However, traditional direct mixing processes face four technical bottlenecks.

Physicochemical Stability Deficiency: The mixed system tends to experience alkali return during use, causing significant fluctuations in micro-area pH values within the range of 8.5–11.5 [10,11], which affects the stability of plant growth. Environmental Risk Hazards: Secondary release of soluble phosphorus and fluorine from phosphogypsum [12] may lead to water eutrophication and soil fluorine pollution. Heavy Metal Activation Risk: Heavy metals such as Pb, Cd, and As in industrial waste are prone to desorption and migration under acidic conditions, posing threats to ecological safety [11]. Substrate Function Deficiency: The primary pores in the original mixed material are mostly micropores, with porosity below 30%, resulting in poor water and nutrient retention capacity, limiting plant root development [13].

In recent years, researchers have explored various approaches to utilize RM and PG. RM has been employed for soil remediation and wastewater treatment due to its porous structure and heavy metal adsorption properties [14]. PG, rich in nutrients such as sulfur and phosphorus, has been tested for soil improvement and construction materials [15]. However, the strong alkalinity of RM and the strong acidity of PG limit their direct application. Although their combined use can neutralize acid–base effects, the resulting mixture is often unstable [16], posing risks of secondary pollution, such as the leaching of phosphorus, fluoride, and heavy metals.

To address these challenges, researchers have conducted extensive studies on the modification of RM and PG. For instance, Xu et al. [17] used ferric chloride ($FeCl_3$) as a pH regulator for RM, successfully stabilizing its alkalinity at around 8.5 within 30 days. Han [18] prepared dealkalized modified RM by mixing lime and $FeCl_3$ with dry RM residue, demonstrating its effectiveness in reducing environmental risks. On the other hand, Ji et al. [19] used sodium silicate (Na_2SiO_3) as a PG stabilizer, altering the hydrophilic–hydrophobic properties of PG particles and improving their water stability. Zemni et al. [20] found that treating PG with Na_2SiO_3 could recover calcium silicate and significantly reduce the release of free calcium, further enhancing its environmental safety. Liu et al. [21] demonstrated that the artificial soil prepared from red mud and phosphogypsum exhibited significant enrichment in the community structure of nitrogen-fixing bacteria and cellulose-decomposing bacteria. These microorganisms effectively enhanced the fertility of the artificial soil by increasing soil organic matter content and promoting nutrient cycling and energy flow, thereby activating the biological activity of the soil ecosystem.

Despite these advancements, there is a lack of comprehensive studies on the synergistic effects of combining modified RM and PG for soil and ecological remediation. Previous research has primarily focused on individual modifications of RM or PG, with limited exploration of their combined application. Moreover, the mechanisms underlying the immobilization of toxic ions (e.g., phosphorus, fluoride, and heavy metals) in RM-PG composites remain poorly understood. Therefore, there is a pressing need to develop innovative composite materials that can effectively utilize RM and PG while minimizing their environmental risks.

Based on these research gaps, this study proposes an innovative composite substrate preparation method that involves the modification of red mud and phosphogypsum using ferric chloride and sodium silicate, respectively. Perennial ryegrass (Lolium perenne), characterized by its broad environmental adaptability [22], rapid growth rate, high biomass accumulation capacity, and notable tolerance and accumulation capacity for heavy metals [23], was selected as the experimental plant for pot experiments. The primary objectives of this study are (1) to investigate the regulatory effects and mechanisms of ferric chloride and sodium silicate modifiers on the physicochemical properties of RM and PG; (2) to optimize the ratio of the RM-PG composite substrate and evaluate its application effects in terms of microstructure and heavy metal control; and (3) to verify the long-term environmental risks and ecological effects of the composite substrate through perennial ryegrass pot experiments. By addressing these research objectives, this study aims to provide scientific evidence for the application of RM-PG composites in land ecological restoration projects, and contribute to the sustainable utilization of industrial solid wastes.

2. Materials and Methods

2.1. Materials

The red mud was sourced from a red mud disposal site in Kaili City, Guizhou Province (26°38′ N, 107°48′ E). It appears as reddish-brown blocks with a pH of 10.76 and a moisture content of 28%. The phosphogypsum was obtained from a phosphogypsum disposal site at the Wengfu Phosphate Mine in Guizhou Province, exhibiting a grayish-black appearance with a moisture content of 17%. Both materials were dried in the dark under natural conditions, ground, and sieved (60 mesh) for subsequent use. Ultrapure water was used for all experimental procedures. The primary chemical properties of red mud and phosphogypsum, as determined by X-ray fluorescence spectroscopy (XRF) (Table 1), indicate that the main oxides in phosphogypsum are SO_3 and CaO, while red mud is predominantly composed of Fe, Al, Si, and Ca oxides, collectively accounting for over 90 wt.% of the total mass. X-ray diffraction (XRD) analysis (Figure 1) revealed that the primary phases in red mud include gibbsite, hematite, and perovskite, whereas phosphogypsum is mainly composed of gypsum and apatite minerals. Microstructural morphology analysis showed that the crystal structure of red mud (Figure 2a) is characterized by dispersed particles with varied shapes and rough surfaces, while phosphogypsum (Figure 2b) primarily exhibits a plate-like structure, forming a relatively dense configuration. BET analysis (Table 2) indicated that phosphogypsum has a large specific surface area with numerous active sites, whereas red mud possesses large pore sizes and high pore volume, making it suitable for macromolecular adsorption. Leachate analysis (Table 3) demonstrated that the concentrations of heavy metals in both materials meet the requirements of the "Integrated Wastewater Discharge Standard" (GB8978-1996 [24]). However, the strong alkalinity of red mud and the strong acidity of phosphogypsum, along with its high phosphate and fluoride ion content, necessitate attention to potential environmental risks.

Table 1. Chemical composition of the slag material (wt.%).

Material	SO_3	CaO	SiO_2	P_2O_5	Al_2O_3	Fe_2O_3	Na_2O	Others
Red Mud	1.89	16.12	18.16	0.15	22.22	24.61	10.48	6.37
Phosphogypsum	52.19	39.29	4.99	1.42	0.54	0.27	0.15	1.15

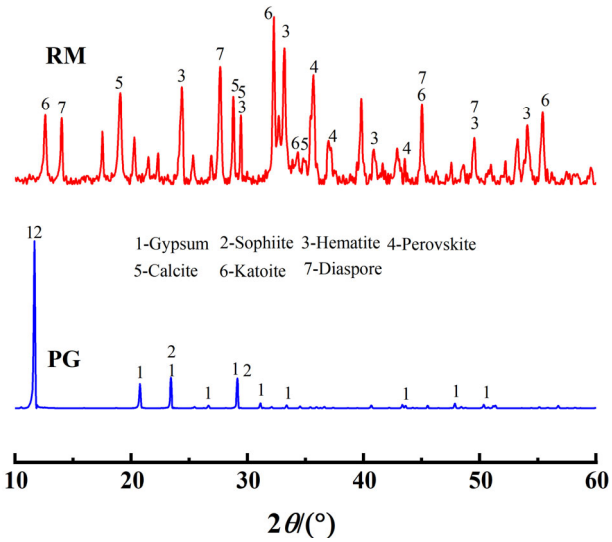


Figure 1. XRD Patterns of red mud and phosphogypsum.

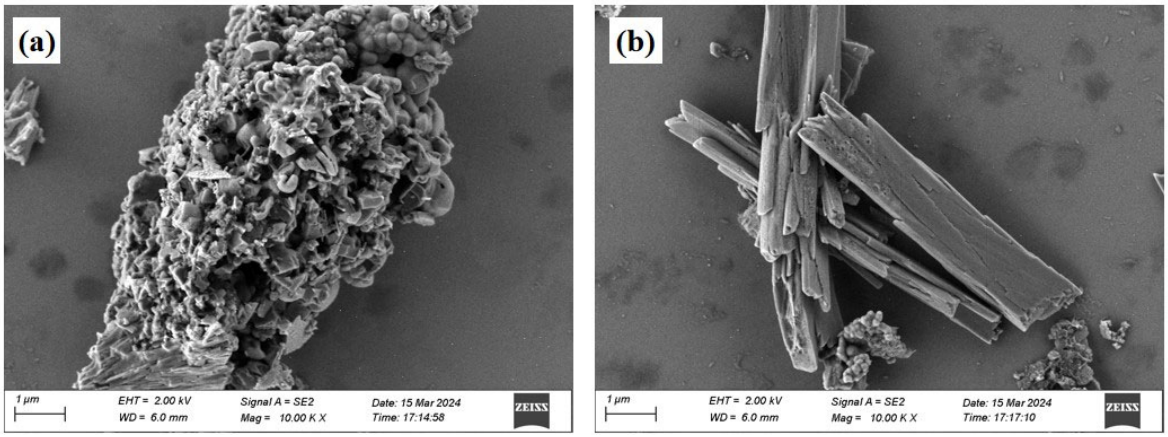


Figure 2. SEM images of red mud (**a**) and phosphogypsum (**b**).

Table 2. Specific surface area, pore diameter, and pore volume of red mud and phosphogypsum.

Material	Specific Surface Area/($m^2 \cdot g^{-1}$)	Aperture/(nm)	Pore Capacity/($cm^3 \cdot g^{-1}$)
Red Mud	14.465 ± 0.27	25.494 ± 1.72	0.0921 ± 0.002
Phosphogypsum	17.737 ± 0.32	14.043 ± 0.47	0.0622 ± 0.010

Table 3. Leaching toxicity of slag materials (mg/L).

Material	pH	PO_4^{3-}-P	F^-	Zn	Cd	As	Cu	Mn	Ni
RM	10.76	0.06	4.61	0.015	-	0.047	0.009	0.006	0.006
PG	3.38	205.7	48.49	0.28	0.002	0.32	0.077	1.22	0.06
GB8978-1996	6–9	≤0.5 (I)	≤10 (I)	≤2.0 (I)	≤0.1	≤0.5	≤0.5 (I)	≤2.0 (I)	≤1.0

Note: "-" indicates below the detection limit; "(I)" indicates the Class I standards of the GB8978-1996.

2.2. Modification Experiment

The modification process involved the application of 0.5 mol/L and 1 mol/L $FeCl_3$ reagent (FC) at varying mass ratios (5%, 10%, and 15%) to spray-treat the red mud. Concurrently, phosphogypsum was treated by spraying with 1.4 mol/L Na_2SiO_3 reagent, as referenced in previous studies [25,26]. The treated materials were thoroughly mixed and

aged for 24 h to yield the modified products, designated as FRMa/FRMb (for red mud) and NPG (for phosphogypsum). The detailed experimental protocol for the modification process is comprehensively outlined in Table 4.

Table 4. FRM and NPG trial protocol design.

Processing Group	Matter	Material Weight (g)	Reagent Concentration (mol/L)	Use of Modified Reagent (wt.%)
RM	Red mud	100	No treatment	/
PG	Phosphogypsum	100	No treatment	/
FRMa	Ferric chloride modified red mud a	100	0.5 mol/L $FeCl_3$	5% 10% 15%
FRMb	Ferric chloride-modified red mud b	100	1 mol/L $FeCl_3$	5% 10% 15%
NPG	Sodium silicate-modified phosphogypsum	100	1.4 mol/L Na_2SiO_3	5% 10% 15%

Ultrapure water, equivalent to 10% of the total admixture by mass, was sprayed onto the materials to maintain moisture and ensure homogeneous mixing. The material was then spread evenly and allowed to age at room temperature for 24 h. The mixture was thoroughly blended according to the specified mass ratios. The detailed experimental design for the testing procedure is provided in Table 5.

Table 5. Experimental design of red mud and phosphogypsum modified complex.

Processing Group	T1			T2			T3			T4			T5		
FRMa (15%)	30	/	/	40	/	/	50	/	/	60	/	/	70	/	/
FRMb (10%)	/	30	/	/	40	/	/	50	/	/	60	/	/	70	/
FRMb (15%)	/	/	30	/	/	40	/	/	50	/	/	60	/	/	70
NPG (10%)	70	70	70	60	60	60	50	50	50	40	40	40	30	30	30
Total	100	100	100	100	100	100	100	100	100	100	100	100	100	100	100

Note: "/" means not added.

2.3. Pot Experiment

The FRMb (15%) and NPG (10%) were mixed at mass ratios of 7:3, 6:4, and 5:5, respectively. To each mixture, pure water equivalent to 10% of its total mass was added to ensure sufficient moisture and uniform mixing. The three treatment groups were designated as FN1, FN2, and FN3 based on their respective mass ratios, while untreated soil served as the control group (CK). A ryegrass cultivation experiment was conducted using the aforementioned treatment groups as the planting substrate.

For each treatment, 500 g of the mixed and aged material was placed into pots measuring 10 cm in diameter and 9 cm in height. Subsequently, 100 ryegrass seeds were evenly sown in each pot. The pots were watered and maintained to ensure the substrate moisture content remained at 60–70% of field water retention capacity. Each treatment group was replicated three times to ensure statistical reliability.

Based on the research conducted by Xing et al. [27], the phytoremediation efficacy was evaluated by analyzing the physicochemical properties of the pot leachate, as well as the fresh weight and plant height of ryegrass. To evaluate the long-term vegetation

restoration potential of the modified composite materials, the planting experiment was conducted over a 45-day period. Germination rates were calculated, and plant height and chlorophyll content were measured at 20 days and 40 days, respectively. At the 40-day mark, leachate samples were collected from both the control and treated groups for analysis of pH, electrical conductivity (EC), phosphate (PO_4^{3-}), and fluoride (F^-) concentrations. After 45 days, the aboveground biomass from each pot was harvested and dried to determine dry weight.

2.4. Index Detection and Determination Methods

The leaching procedure was conducted in accordance with the "Solid Waste Extraction Method" (HJ 557-2010 [28]), employing a solid–liquid ratio of 1:10. The oscillation frequency was maintained at 110 ± 10 times per minute with an amplitude of 40 mm, and the extraction process was carried out for 16 h, including 8 h of oscillation. The supernatant was collected from both the extract and potting leachate for subsequent analysis. The pH value was measured using a PHS-3C pH meter, while the electrical conductivity (EC) was determined using an EC-30 pen conductivity meter. The concentrations of phosphate (PO_4^{3-}) and fluoride (F^-) were quantified following the "Determination of Total Phosphorus in Water Quality by Ammonium Molybdate Spectrophotometry" (GB 11893-1989 [29]) and the "Determination of Fluoride in Water Quality by Fluoride Ion Selective Electrode Method" (GB 7484-1987 [30]), respectively. Additionally, the heavy metal content in the leaching solution was analyzed.

The chemical composition and mass ratios of red mud, phosphogypsum raw slag, and the compound admixture were determined using an X-ray fluorescence spectrometer (XRF) (Rigaku ZSX Primus III+, Toyohashi, Aichi, Japan). The specific surface area, pore volume, and pore size distribution of the materials before and after modification were analyzed using the Brunauer–Emmett–Teller (BET) method (Micromeritics ASAP 2460, Norcross, GA, USA). The crystalline phases of the materials were identified using an X-ray diffractometer (XRD) (Rigaku Ultima IV, Toyohashi, Aichi, Japan). The microstructural morphology of the waste materials before and after modification was observed using scanning electron microscopy (SEM) (ZEISS Sigma 300, Oberkochen, Hesse, Germany). The concentrations of heavy metals, including manganese (Mn), zinc (Zn), cadmium (Cd), and lead (Pb), were detected using inductively coupled plasma mass spectrometry (ICP-MS) (PerkinElmer NexION 300×, Waltham, MA, USA). All analytical procedures were performed in triplicate to ensure reproducibility and accuracy.

3. Results

3.1. $FeCl_3$ Regulation of pH and EC Values in Red Mud

As indicated in Table 3, the leachate from red mud complies with the requirements of the "Integrated Wastewater Discharge Standard" (GB8978-1996). Therefore, the evaluation of red mud degradation primarily focuses on pH and electrical conductivity. Figure 3 presents a comparative analysis of the pH and EC values between the modified red mud (FRM) and untreated red mud slag, following treatment with 0.5 mol/L and 1 mol/L $FeCl_3$ solutions at varying mass ratios.

The pH of FRM decreased from an initial value of 10.67 to a range of 8.51–10.05, demonstrating that the $FeCl_3$ spray treatment effectively reduced the alkalinity of the red mud. This reduction in pH became more pronounced with increasing concentration and incorporation rate of the $FeCl_3$ solution. Concurrently, due to the introduction of Fe^{3+} and Cl^- ions from the modifying agent, the EC of the FRM material increased from 0.74 mS/cm to a range of 1.23–4.81 mS/cm, exhibiting a consistent upward trend. These

results highlight the dual effect of $FeCl_3$ modification: mitigating the alkalinity of red mud while increasing its ionic conductivity due to the incorporation of additional ions.

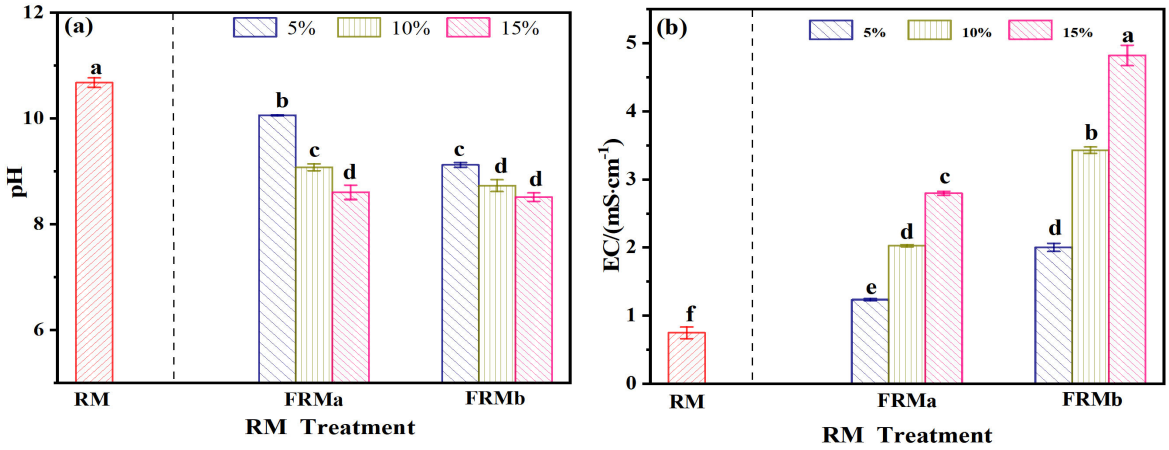


Figure 3. $FeCl_3$ and the effect of usage on red mud pH (**a**) and EC (**b**). Note: different superscript letters in the same row indicate significant differences ($p < 0.05$).

The interaction of iron (III) with alkaline anions present in RM within an aqueous environment, along with the subsequent dehydrogenation process leading to the formation of colloidal particles, can be described by the following series of reactions, as represented by Equation (1) through Equation (5) [31]. The rate of hydrolysis in this process is governed by the molar ratio of Fe^{3+} to hydroxide ions (OH^-) [32].

These reactions illustrate the chemical transformation of Fe^{3+} in the presence of alkaline components in red mud, ultimately resulting in the formation of colloidal iron hydroxides. The hydrolysis rate is highly dependent on the relative concentrations of Fe^{3+} and OH^-, which influence the kinetics and extent of the reaction.

$$Fe^{3+} + OH^- \rightarrow Fe(OH)_3 \downarrow \quad (1)$$

$$Fe^{3+} + H_2O + CO_3^{2-} \rightarrow Fe(OH)_3 \downarrow + CO_2 \uparrow \quad (2)$$

$$Fe^{3+} + HCO_3^- \rightarrow Fe(OH)_3 \downarrow + CO_2 \uparrow \quad (3)$$

$$Fe^{3+} + H_2O \overset{-H^+}{\rightarrow} FeOH^{2+} + Fe_2(OH)_2{}^{4+} + Fe(OH)_2{}^{+} \quad (4)$$

$$H^+ + Al(OH)_4^- \rightarrow Al(OH)_3 \downarrow + H_2O \quad (5)$$

Under the influence of iron salt treatment, the strong alkalinity of RM was effectively mitigated. In the treatment groups, specifically FRMa (15%), FRMb (10%), and FRMb (15%), the pH decreased from an initial value of 10.76 to a range of 8.51–8.72. This reduction confirms the efficacy of iron salt spraying in regulating the alkalinity of red mud. The iron salt facilitates the dissolution of Ca^{2+} and Na^+ ions present in RM, which are subsequently replaced by Fe^{3+} ions in the solution [13]. This ion exchange process contributes to the observed increase in the EC of the leachate, which correlates with both the concentration and incorporation rate of the iron salt.

EC serves as a critical indicator of salt content, and excessive addition of iron salt should be avoided to prevent the risk of soil salinization during red mud remediation. Under the single ferric chloride treatment, the pH values of the aforementioned treatment groups fall within the permissible range specified by the "Integrated Wastewater Discharge Standard" (GB8978-1996), which mandates a pH range of 6–9. This demonstrates that the treatment not only effectively reduces alkalinity, but also ensures compliance with regulatory standards for wastewater discharge.

3.2. Na_2SiO_3 Regulation on PO_4^{3-} and F^- in Phosphogypsum

Phosphogypsum provides essential nutrients for vegetation growth, and its traditional application involves utilizing its strong acidic components to neutralize the exposed lattice and crystal bases on the surface of red mud particles [31], thereby adjusting the alkalinity of the system. The incorporation of even a small amount of PG is sufficient to regulate the alkalinity of modified red mud (FRM). However, the overall composite remains deficient in nutrients. To address this, sodium silicate-modified PG aims to inhibit the leaching of harmful phosphorus and fluorine while activating the beneficial components of PG. This approach allows for an increased dosage of PG, thereby enriching the nutrient content of the composite material.

As illustrated in Figure 4, the effects of varying doses of sodium silicate treatment on the pH, EC, and the leaching of phosphorus and fluorine from phosphogypsum were evaluated. Following treatment, both pH and EC exhibited a linear increase with the volume of Na_2SiO_3 reagent. The pH rose from 3.38 to a range of 4.89–9.54, while EC increased from 1.37 mS/cm to 2.09–3.49 mS/cm. Conversely, the leaching of phosphorus and fluorine decreased steadily with increasing Na_2SiO_3 dosage. The PO_4^{3-} content decreased from 205.7 mg/L to 0.45–150.9 mg/L, and the F^- content decreased from 48.49 mg/L to 1.69–23.73 mg/L.

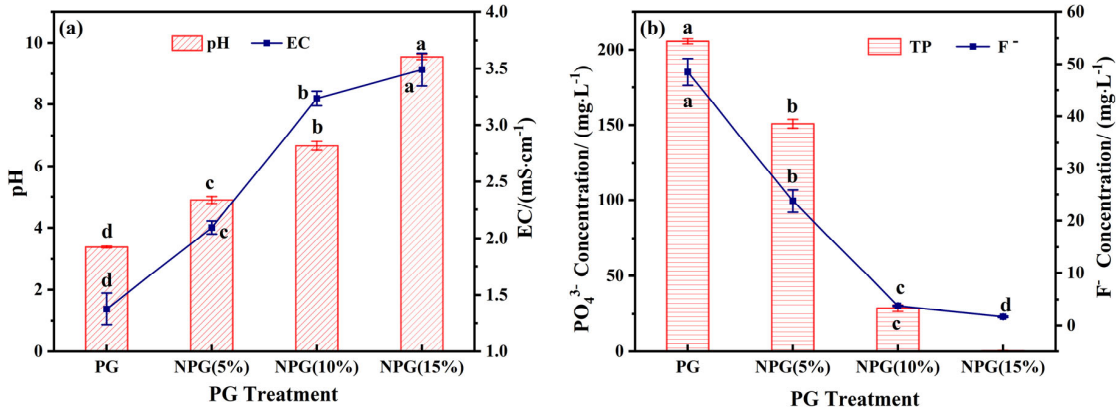


Figure 4. Effect of sodium salt incorporation on pH and EC (**a**), PO_4^{3-}, and F^- (**b**) concentrations of phosphogypsum. Note: different superscript letters in the same row indicate significant differences ($p < 0.05$).

Compared to the original phosphogypsum residue, the PO_4^{3-} and F^- content in the NPG (10%) treatment group decreased by 86% and 92%, respectively, while the pH value increased from 3.38 to 6.67. These results demonstrate that Na_2SiO_3, acting as a modifier, effectively enhances the alkalinity of PG and significantly regulates the release of phosphorus and fluoride. Based on these findings, NPG (10%) is identified as the optimal choice for the preparation of composite materials.

3.3. Leaching Toxicity of Modified Complex

Based on the prior analysis of modified red mud (FRM) and sodium silicate-treated phosphogypsum (NPG), NPG (10%), FRMa (15%), FRMb (10%), and FRMb (15%) were selected for the preparation of composite materials. These two materials were mixed in varying ratios, and the resulting extracts were used for toxicity analysis of the composite admixture.

Acidity and alkalinity significantly influence the surface charge of composite materials, which is a critical factor in the removal of harmful pollutants at the water–material interface. Additionally, pH plays a vital role in determining the availability of nutrient elements within the composite material. As shown in Figure 5a, the pH of the FRM-NPG composite

exhibited a slight increase, ranging between 7.5 and 8.21. This pH shift is attributed to the increased proportion of red mud, which reacts with acidic ions in phosphogypsum to form neutral salts. Furthermore, the free Ca^{2+} ions in phosphogypsum can inhibit the dissolution of alkaline components in red mud [32], thereby enabling effective pH control of the composite admixture.

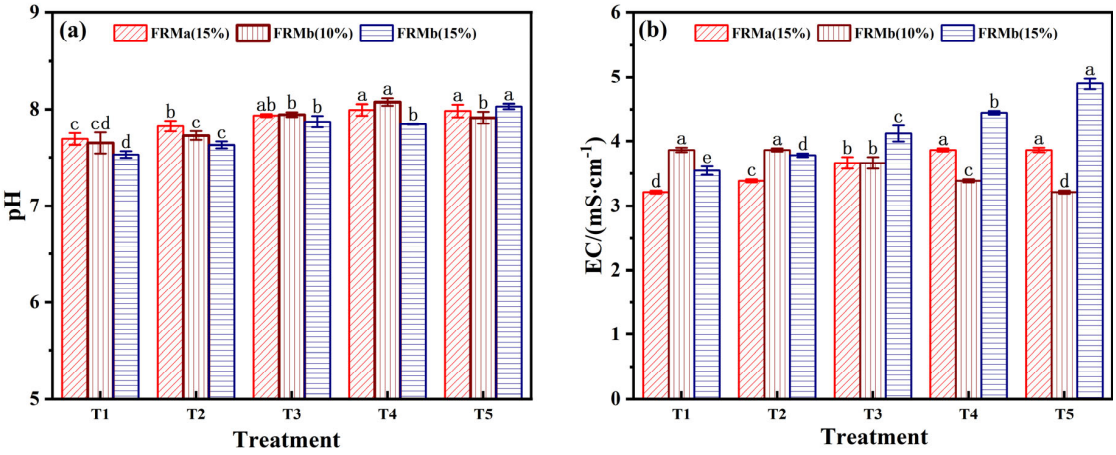


Figure 5. Effect of different ratios of compound admixtures on pH (**a**) and EC (**b**). Note: different superscript letters in the same row indicate significant differences ($p < 0.05$).

The Ca^{2+} ions in phosphogypsum can react with CO_3^{2-}, HCO^{3-}, OH^-, and $Al(OH)^{4-}$ present in red mud to form precipitates such as calcite ($CaCO_3$), calcium hydroxide ($Ca(OH)_2$), and calcium aluminate ($Ca_3Al_2(OH)_{12}$) [33]. These reactions help maintain the pH and Al^{3+} content of the composite at levels conducive to plant growth. As a result, the pH of the modified composite is stabilized under near-neutral conditions, ensuring an environment suitable for vegetation restoration and minimizing potential environmental risks.

EC, as a critical parameter reflecting the salt concentration of the matrix, directly influences nutrient and water absorption during ecological restoration processes [34]. As observed in Figure 5b, the EC values of the FRM-NPG composite increased within the range of 3.21–4.89 mS/cm across different mixing ratios. Notably, the T5 treatment group, which utilized FRMb (15%), exhibited the highest conductivity. This change in EC reflects the dynamic adjustment of Na^+ and Ca^{2+} concentrations in the leaching solution. Specifically, Ca^{2+} released from NPG promotes the precipitation of basic anions, while Ca^{2+}, Na^+, and Fe^{3+} on the material surface undergo active ion exchange in the solution [35].

PO_4^{3-} is a key pollutant associated with phosphogypsum utilization. While phosphorus is an essential nutrient for the environment, exceeding the threshold of environmental tolerance can disrupt the ecological balance between soil and groundwater. The changes in phosphorus concentration across different treatment groups were investigated through leaching tests. As shown in Figure 6a, the phosphorus content in the leaching solution exhibited a stable decrease with increasing FRM incorporation. At a 70% incorporation rate, the T5 treatment group, which utilized FRMb (15%), successfully controlled the total phosphorus (TP) concentration at 0.36 mg/L, meeting the Level I standard for PO_4^{3-} content ($PO_4^{3-} < 0.5$ mg/L).

The phosphorus removal mechanism of FRM primarily relies on three components: Ca, Fe, and Al [36]. In an aqueous medium, these elements form insoluble or low-solubility salts, such as calcium phosphate and aluminum phosphate, upon binding with phosphate. This process fixes the phosphate in the form of solid-phase precipitates, effectively controlling the phosphorus content in the extract. This mechanism highlights the potential of FRM-based composites for mitigating phosphorus pollution while supporting ecological restoration efforts.

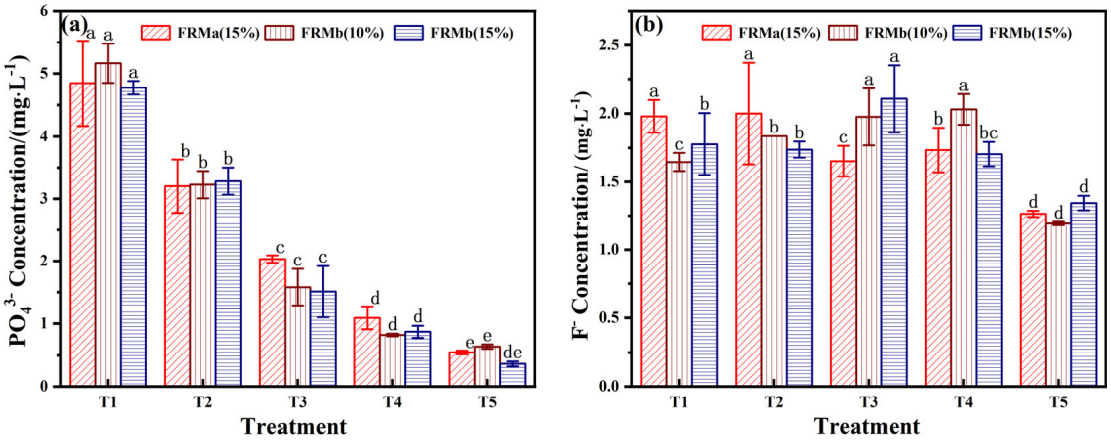


Figure 6. Effect of different blending ratios on PO_4^{3-} (**a**) and F^- (**b**) concentrations. Note: different superscript letters in the same row indicate significant differences ($p < 0.05$).

The fluoride ion concentration in bauxite slag extract can reach up to 11.5–26.7 mg/L [37], while the fluorine content in phosphogypsum, originating from phosphate ore, accounts for 20–40% of its composition [38]. Given that fluoride ion leaching is a primary contributor to environmental fluorine pollution and endemic fluorosis, strict monitoring of fluoride ion concentration is essential during the preparation of composites from phosphogypsum and red mud.

As illustrated in Figure 6b, the F^- concentration in the FRM-NPG composite remained relatively stable within the range of 1.2–2.2 mg/L, which complies with the wastewater discharge standard of F^- content below 10 mg/L. Notably, when the FRM ratio reached 70%, the F^- concentration decreased to its lowest level of approximately 1.2 mg/L. This reduction can be attributed to the electrostatic adsorption of fluoride ions by the positively charged surfaces of FRM, a process that follows a quasi-second-order kinetic model [39]. Additionally, ion exchange processes on the material surface further contribute to fluorine removal.

Considering the combined evaluation of pH, EC, PO_4^{3-}, and F^- content, the T5 treatment group, which combines FRMb (15%) and NPG (10%) at a 7:3 mass ratio, emerges as the optimal formulation. This combination effectively balances alkalinity regulation, nutrient enrichment, and pollutant control, making it suitable for ecological restoration applications.

3.4. Microscopic Analysis of Modified Red Mud–Phosphogypsum Composites

Specific surface area, pore volume, and pore size are critical parameters for characterizing materials, as their changes significantly influence the adsorption capacity and reactivity of composites. Table 5 summarizes the variations in specific surface area, pore size, and pore volume of RM, PG, and composite materials under different treatment conditions. After treatment with ferric chloride, the specific surface area of FRMb (15%) increased by 8.71%, while the pore size decreased by 55.06%, and the pore volume decreased by 42.57%. This indicates that $FeCl_3$ treatment significantly enhanced the surface active sites of red mud, thereby improving its adsorption capacity for pollutants. The reduction in pore size suggests that the modified red mud is more suitable for adsorbing small-molecule pollutants, although the decreased pore volume may limit its capacity for large-molecule pollutants.

In contrast, after treatment with Na_2SiO_3, the specific surface area and pore volume of NPG (10%) increased by 7.44% and 5.62%, respectively, while the pore size decreased by only 1.73%. This demonstrates that Na_2SiO_3 treatment further optimized the microstructure of phosphogypsum, increasing its surface activity while minimally affecting its pore structure and slightly enhancing its pore volume.

Compared to the T5 control group (RM (70%) + PG (30%)), the specific surface area and pore volume of the T5 treatment group (FRMb (15%)) increased by 48.9% and 6.5%, respectively, while the pore size decreased by 28.6%. These results indicate that the modification treatment significantly enhanced the specific surface area, optimized the pore structure, and provided a better balance for adsorbing pollutants of varying molecular sizes. Furthermore, the increased pore volume of the composite material improved its overall adsorption capacity, demonstrating its effectiveness in adsorbing pollutants of different molecular sizes.

Figure 7 compares the X-ray diffraction (XRD) patterns of the T5 control group and the T5 treatment group composite materials. In the XRD pattern of the T5 control group, the diffraction peaks of gypsum and brushite, two primary mineral components, are clearly observed. In the modified composite material, new diffraction peaks corresponding to iron di(2,3,4-trihydroxybutyrate) hydrate and iron molybdenum fluoride appear, indicating the introduction of iron-based compounds during the modification process. Simultaneously, the diffraction peaks of certain minerals weakened or disappeared after modification, further demonstrating the alteration of the mineral composition due to the treatment. Notably, the introduction of iron-based compounds likely contributes to the immobilization of harmful substances (such as phosphorus and fluorine) within the composite material and promotes mineral transformation and recrystallization, thereby reducing its potential environmental risks.

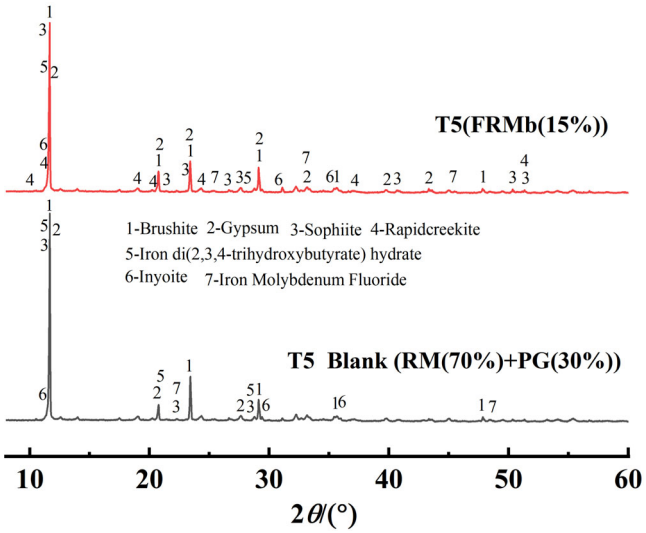


Figure 7. Comparison of XRD Patterns for Modified Composite Materials.

Combined with the Brunauer–Emmett–Teller (BET) analysis results presented in Table 6, it can be concluded that the modification treatment not only optimized the pore structure of the composite material but also improved its surface properties, significantly enhancing its adsorption capacity and reactivity. These findings underscore the effectiveness of the modification process in tailoring the composite material for environmental remediation applications.

In the control group (Figure 8a), the particles exhibit irregular shapes, rough surfaces, and large pores, with an overall loose and porous stacking structure. This morphology is characteristic of untreated materials, where the lack of modification results in a less organized and less dense arrangement of particles. In contrast, the modified composite material (Figure 8b) demonstrates more regular crystal particle shapes, improved surface smoothness, and a denser pore structure. These changes can be attributed to the modification treatment, which promotes the recrystallization process and surface modification of the

particles. The regularization of particle shapes and the enhancement of surface smoothness indicate that the treatment facilitates the reorganization of the material at the microscopic level, leading to a more uniform and compact structure.

Table 6. Specific Surface Area, Pore Diameter, and Pore Volume of red mud, phosphogypsum, and Composite Materials under Different Treatment Conditions.

Processing Group	Specific Surface Area/($m^2 \cdot g^{-1}$)	Aperture/(nm)	Pore Capacity/($cm^3 \cdot g^{-1}$)
FRMb (15%)	15.725 ± 0.09 b	16.441 ± 0.83 b	0.0646 ± 0.001 c
NPG (10%)	19.053 ± 0.53 a	13.804 ± 0.56 d	0.0657 ± 0.002 b
T5 Blank (RM (70%) + PG (30%))	11.366 ± 0.20 c	22.192 ± 1.52 a	0.0630 ± 0.003 d
T5 (FRMb (15%))	16.945 ± 0.86 b	15.849 ± 0.16 bc	0.0671 ± 0.001 a

Note: different superscript letters in the same row indicate significant differences ($p < 0.05$).

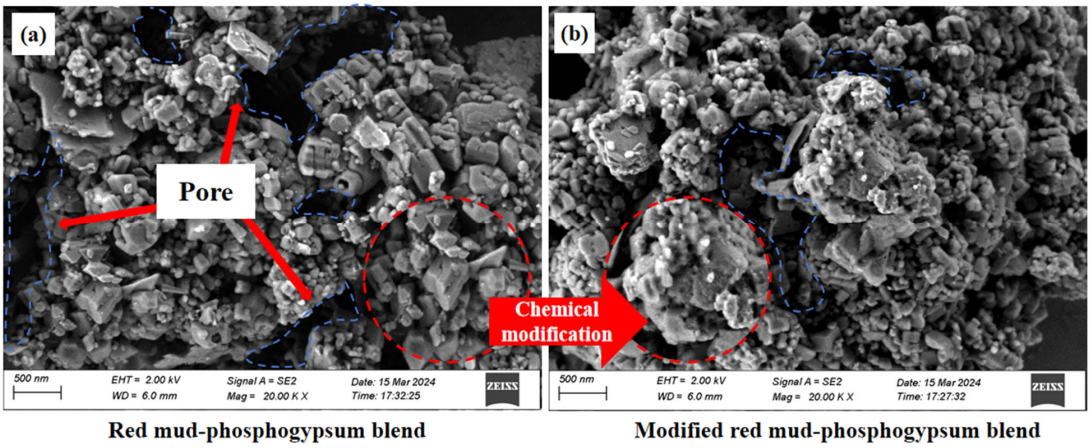


Figure 8. Comparison of SEM Images of Composite Materials Before (**a**) and After Modification (**b**).

The modification treatment optimizes the composite material's pore structure, as indicated by reduced pore size and increased packing density. This enhances adsorption capacity and reactivity by providing more active sites for pollutant adsorption and chemical reactions. Smoother surfaces and tighter interparticle connections improve surface properties, stability, and mechanical strength. Scanning electron microscopy (SEM) images visually illustrate these microscopic changes, serving as auxiliary validation of the chemical modification. The observed morphological changes align with the increased specific surface area and optimized pore volume shown in Table 6, confirming a more compact microstructure and enhanced particle aggregation. These findings demonstrate the modification's effectiveness in improving the material's structural and functional properties, making it more suitable for environmental remediation applications.

3.5. Analysis of the Characteristics of Heavy Metals in the Modified Red Mud–Phosphogypsum Composite Material

Heavy metal elements carried by industrial waste residues, once dissolved, pose significant risks to soil fertility, water environment safety, and crop growth. Mn, Zn, Cd, Pb, Cu, and Ni are among the primary heavy metal pollutants identified in the leachate from red mud and phosphogypsum storage yards [40,41]. The results of heavy metal content analysis in the FRM-NPG composite extract are presented in Figure 9. The concentrations of heavy metals in the leachate of both unmodified red mud and phosphogypsum meet the maximum allowable discharge concentration requirements specified in the "Integrated Wastewater Discharge Standard" (GB8978-1996). In the treatment groups, the concentrations of heavy metals were effectively reduced compared to the original waste residues,

and no increase in heavy metal concentration was observed due to the incorporation of the composite materials.

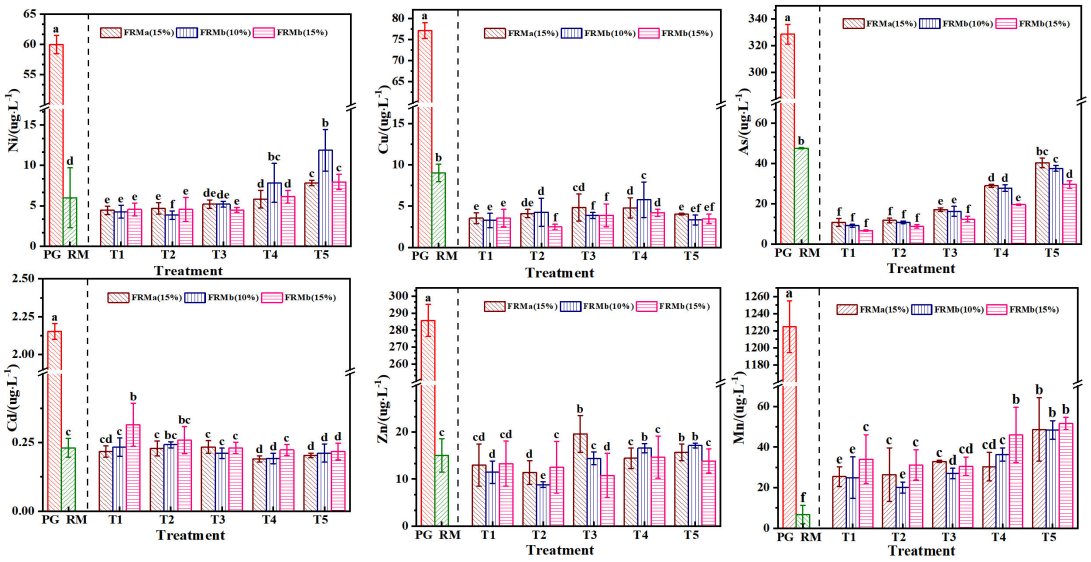


Figure 9. Effect of different ratios of compound admixture on heavy metal concentration. Note: different superscript letters in the same row indicate significant differences ($p < 0.05$).

Specifically, the concentrations of Ni, Mn, and As increased with higher incorporation rates of NPG, while the concentrations of Cd, Cu, and Zn were less influenced by the proportion of NPG in the composite. This suggests that the modification process and the interaction between FRM and NPG play a significant role in immobilizing certain heavy metals, thereby reducing their leaching potential. However, the behavior of Ni, Mn, and As indicates that their mobility may be influenced by the chemical environment created by the composite materials. These findings highlight the importance of carefully optimizing the composition and modification of waste-derived composites to minimize the environmental risks associated with heavy metal leaching. The effective reduction in heavy metal concentrations in the treatment groups demonstrates the potential of FRM-NPG composites for safe environmental applications, provided that the specific interactions and leaching behaviors of individual heavy metals are thoroughly understood and managed.

The effective reduction in heavy metal content in each treatment group is primarily attributed to the sulfate present in phosphogypsum, which promotes the formation of calcium silicate hydrate (C-S-H) gel and ettringite (AFt) under the activation of SiO_2, Al_2O_3, and CaO from red mud. This process accelerates the dissolution of both red mud and phosphogypsum, leading to an increased release of silicate, aluminate, and Ca^{2+} ions [42]. The stabilization of heavy metals in the composite admixture is achieved through a combination of physical encapsulation, adsorption, isomorphic replacement, and precipitation curing. The formation of C-S-H gel and ettringite encapsulates heavy metal ions, preventing their release into the environment, while the high surface area and active sites of the composite materials facilitate the adsorption of heavy metal ions. Additionally, heavy metal ions may replace Ca^{2+} or other ions in the crystal lattice of C-S-H gel or ettringite through isomorphic replacement, effectively immobilizing them [43]. Furthermore, heavy metals form insoluble compounds, such as calcium silicate gels and calcium vanadate, through precipitation reactions, further reducing their mobility. These mechanisms collectively contribute to the stabilization of heavy metals within the composite admixture, minimizing their leaching potential and environmental risks, thereby demonstrating the effectiveness of the FRM-NPG composite in immobilizing heavy metals and highlighting its potential for safe environmental applications.

3.6. Potting Experiment

Based on the study of modified composites, FRMb (15%) and NPG (10%) were selected and mixed in different ratios (7:3, 6:4, 5:5) to form three treatment groups: FN1, FN2, and FN3. Fresh soil was used as the blank control group (CK) to evaluate the vegetation restoration potential of the modified red mud–phosphogypsum composite. A 45-day ryegrass pot experiment was conducted to assess the growth performance of the plants in these substrates.

At 40 days, the growth status of ryegrass in the CK, FN1, FN2, and FN3 matrices was recorded, as illustrated in Figure 10. Table 7 summarizes the growth parameters of ryegrass and the physicochemical properties of the CK, FN1, FN2, and FN3 substrates. The results demonstrate that the modified composite materials significantly improved plant growth compared to the control group, with variations in growth parameters such as plant height, chlorophyll content, and biomass depending on the mixing ratio. These findings highlight the potential of the modified red mud–phosphogypsum composite for vegetation restoration, as it provides a favorable growth environment while mitigating the environmental risks associated with the raw materials.

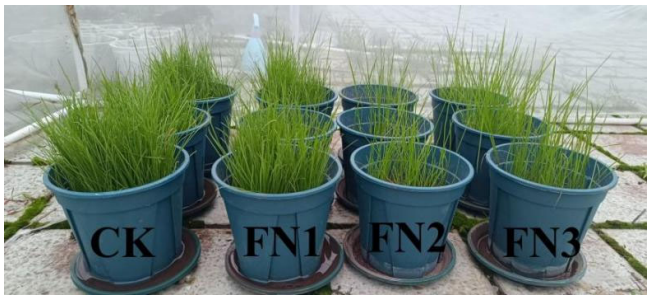


Figure 10. Growth effect of rye grass for 40 days.

The pH values of FN1, FN2, and FN3 remained stable within the range of 8.27 to 8.41, meeting the optimal pH requirements for plant growth [44]. The EC followed the order FN3 > FN2 > FN1 > CK, with all groups maintaining EC values below 4 mS/cm, which is within the safe salinity threshold for plant growth [45]. However, only FN1 met the Grade I requirements for phosphorus and fluorine concentrations in the pot leachate, as specified by the "Integrated Wastewater Discharge Standard" (GB8978-1996). The lower PO_4^{3-} and F^- content in the leachate compared to the modified composite residue may be attributed to the leaching and utilization of these elements during watering and plant growth. The germination rates of ryegrass in the treatment groups were ranked as follows: CK > FN1 > FN2 > FN3. The growth performance of ryegrass in FN1 was comparable to that in fresh soil (CK) after 40 days, with germination rates of 84% and 92%, respectively. In contrast, FN2 and FN3 exhibited modest germination rates of 36% and 34%, respectively. Both plant height and chlorophyll content at 20 and 40 days indicated that ryegrass growth in fresh soil and FN1 was slightly lower than in FN2 and FN3. However, the chlorophyll content in fresh soil and FN1 was significantly higher than in FN2 and FN3. As shown in Figure 10 and Table 7, the aboveground dry weight of ryegrass in FN1 and fresh soil was significantly greater than in FN2 and FN3, further confirming the superior growth performance in these groups. In conclusion, the pot leachate from the modified composite FN1 not only meets the Grade I discharge requirements of GB8978-1996, but also demonstrates ryegrass growth performance comparable to that in fresh soil. These results highlight the potential of FN1 as a viable substrate for vegetation restoration, combining effective pollutant control with favorable plant growth conditions.

Table 7. Growth parameters of ryegrass and the physicochemical properties of the samples.

Group	pH	EC (mS/cm)	PO_3^{4-} (mg/L)	F^- (mg/L)	Germination Percentage (%)	Dry Weight (g)	Plant Height (cm)		Chlorophyll (SPAD)	
							20 d	40 d	20 d	40 d
CK	6.74 ± 0.054 e	0.53 ± 0.020 c	-	-	92.83	21.63 ± 0.05 a	17.36 ± 0.51 b	21.35 ± 0.39 c	58.26 ± 0.61 a	61.15 ± 0.08 a
FN1	8.41 ± 0.039 a	2.41 ± 0.036 a	0.0372 ± 0.030 c	1.049 ± 0.211 c	84.80	18.82 ± 0.06 b	16.60 ± 0.32 c	22.43 ± 0.42 b	55.36 ± 0.61 b	57.92 ± 0.42 b
FN2	8.34 ± 0.025 b	2.77 ± 0.037 b	0.616 ± 0.021 a	2.325 ± 0.034 a	36.43	5.7 ± 0.04 d	17.45 ± 0.33 b	22.15 ± 0.16 b	34.90 ± 0.50 c	41.50 ± 0.79 c
FN3	8.27 ± 0.025 c	2.80 ± 0.136 a	0.492 ± 0.034 b	2.325 ± 0.034 a	34.71	7.31 ± 0.02 c	21.06 ± 0.35 a	23.91 ± 0.34 a	32.96 ± 0.21 d	38.69 ± 0.79 d

Note: "-" means below the detection limit; different superscript letters in the same row indicate significant differences ($p < 0.05$).

4. Discussion

4.1. Effect of pH Change in Red Mud and Phosphogypsum Modified Complex

The pH of the modified composite directly influences the efficiency of phosphorus fixation and fluoride removal. When the pH is between 3 and 5, $H_2PO_4^-$, F^- in the system are less likely to form stable precipitates [46]. In contrast, at a pH range of 7–10, phosphate reacts with calcium, iron, and aluminum in the system to form stable and insoluble metal-phosphate precipitates, which is the primary mechanism of phosphorus fixation in the modified composite [47,48]. Within this pH range, metal ions can also combine with fluoride ions to form insoluble precipitates, thereby achieving effective fluoride removal [48]. Since F^- has a similar ionic radius and charge to OH^-, the hydroxyl ions aggregated on the surface of FRM can react with F^-, further enhancing fluoride removal [49]. However, when the pH exceeds 10, excess OH^- competes with fluoride ions for active sites, leading to a decrease in fluoride removal efficiency [50]. Therefore, the optimal pH range for the modified composite is 7.5–8.2. Additionally, a moderate increase in alkalinity enhances the affinity of electrostatic attraction in the material for negatively charged ions (F^-, HPO_4^{2-}, PO_4^{3-}) [39], thereby improving its phosphorus fixation and fluoride removal capabilities.

As the system pH increases, the Si-O-Si bonds in NPG break, activating Si-O groups and facilitating the formation of more reactive small molecular ions [51]. This promotes the formation of macromolecular substances, such as tricalcium silicate (Ca_3SiO_5) and calcium iron garnet ($Ca_3AlFe(SiO_4)(OH)_8$) complexes. Figure 7 and XRD profile analysis demonstrate the interaction of phosphorus and fluorine with Ca, Fe, Al, and other elements in the composite, resulting in the formation of compounds such as calcium phosphate ($CaPO_3(OH)$), aluminum phosphate ($Al_4(PO_4)_3(OH)_3$), and sodium hexafluoroferrate (Na_3FeF_6). Simultaneously, Al_2O_3 and SiO_2 coat phosphorus–fluoride compounds, forming $Al_2O_3 \cdot P_2O_5$ complexes and calcium iron silicate ($Ca_3Fe_2 \cdot 3(SiO_4)$. Under these alkaline conditions, the modified composite not only reduces the impact of potentially toxic elements (PTEs) in the residue on ryegrass growth, but also minimizes the accumulation of these elements in plant tissues [52]. Furthermore, it enhances the utilization of nutrient elements such as P, S, and Ca from phosphogypsum [53]. The low solubility of NPG ensures the continuous release of calcium ions, which inhibits the alkaline dissolution of the red mud mixture, thereby maintaining the long-term stability of the composite's pH. However, before applying the composite material to environmental remediation, further research is needed to address challenges related to nutrient and alkalinity management, as well as the potential environmental risks posed by heavy metals. These considerations are critical for ensuring the safe and effective use of the modified composite in practical applications.

4.2. Characterization and Reaction Mechanism of the Modified Complex

In the preparation of the FRM-NPG composite admixture, the aqueous medium facilitates the contact and reaction between FRM and NPG particles, as illustrated in Figure 11. The stabilization and immobilization of phosphorus and fluorine primarily occur through the formation of surface precipitates, such as $Ca(PO_4)_2$ and $Ca_5(PO_4)_3F$ [12], as well as inner-sphere complexes achieved via ligand exchange [54]. The residual ferric chloride on the surface of red mud induces coagulation reactions through charge neutralization, generating Fe-F, Fe-P, and other common precipitates [55]. The presence of SO_4^{2-} in the system accelerates the formation of these precipitates and assists in the capture and fixation of phosphorus and fluorine [31].

Changes in pH further promote the formation of calcium silicate hydrate (C-S-H) gel. Under the combined action of $Fe(OH)_3$, $Al(OH)_3$, PO_4^{3-}, F^-, and heavy metal ions are adsorbed and encapsulated within a dense gel matrix, enabling the physical immobilization and co-precipitation removal of harmful substances [56]. C-S-H and ettringite (AFt) possess

large specific surface areas and overlapping interlayer structures, providing abundant active sites for heavy metal adsorption [57]. Additionally, heavy metals can replace Al^{3+} or Ca^{2+} in the lattice of C-S-H and AFt, becoming embedded within their crystalline structures [58]. Calcium ions and sulfate from phosphogypsum can also bind with surface groups on red mud, forming complexes that enhance the adsorption capacity of red mud for heavy metals. This is achieved through Ca^{2+} binding to anions and SO_4^{2-} binding to cations [59]. These mechanisms collectively contribute to the effective stabilization of phosphorus, fluorine, and heavy metals in the FRM-NPG composite, highlighting its potential for environmental remediation applications.

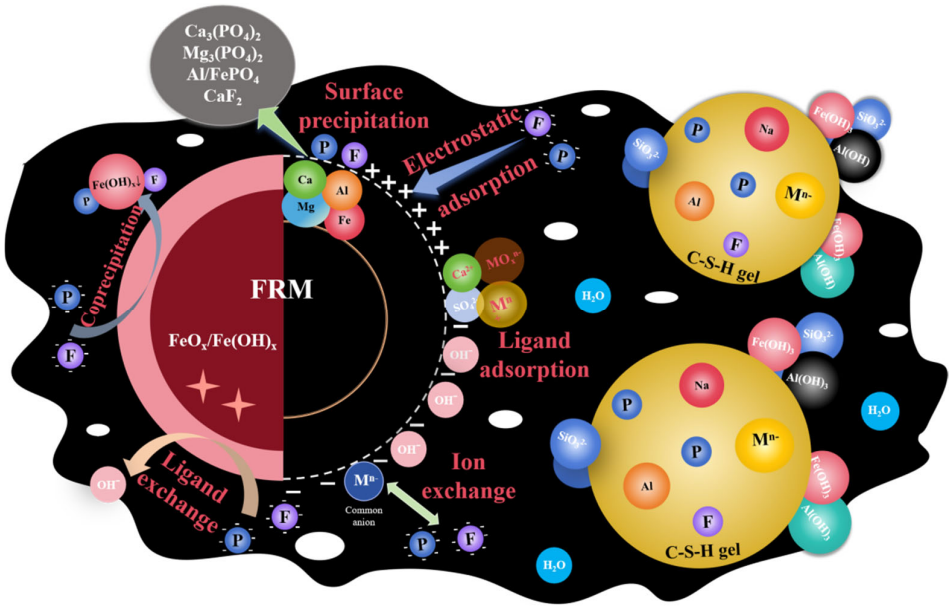


Figure 11. Schematic diagram of the reaction mechanism of modified composite materials.

The alkaline components in red mud are dissolved and removed through reactions with H^+ ions generated by the hydrolysis of iron salts. Initially, Fe^{3+} reacts with alkaline anions (e.g., OH^-, HCO_3^-, $Al(OH)_4^-$) present in red mud to form $Fe(OH)_3$ precipitates and CO_2 gas [60]. Subsequently, the H^+ released from Fe^{3+} hydrolysis reacts with $Al(OH)_4^-$, promoting the formation of $Al(OH)_3$ precipitates [2], while the remaining H^+ continues to neutralize free bases within the system [11]. This process results in an increase in the specific surface area of FRM. Additionally, the incorporation of ferric chloride alters the surface properties of red mud particles and enhances adhesive interactions between particles [38,61]. The formation of $Fe(OH)_x$ gel causes surrounding slag particles to co-precipitate, further modifying the surface properties of the material particles. This process may lead to the blockage of internal pores, reducing pore volume and pore size [62].

The addition of sodium salts promotes the dissolution of phosphogypsum, similar to the disintegration of gypsum, releasing more reactive SiO_2 and Al_2O_3, thereby accelerating the formation of hydration products [63]. This process transforms the originally tightly packed crystal structure of phosphogypsum into a looser configuration, increasing the specific surface area and pore volume of NPG. Simultaneously, the hydrated calcium silicate gel in the system, along with high-surface-area SiO_2, forms a dense gel structure on the outer layer of the particles [64]. This gel fills the granular pores of phosphogypsum and encapsulates or embeds phosphogypsum particles and soluble impurity ions. Although this results in a reduction in pore size, it also strengthens interfacial bonding and adhesion forces among the components [65]. These changes collectively enhance the structural integrity and functional properties of the composite material [66,67], making it more effective for environmental remediation applications.

5. Conclusions

(1) Through a comprehensive evaluation of the growth effects of potted plants and the leaching toxicity test results of the modified composite material, we determined the optimal ratio for the modified red mud–phosphogypsum composite. When the mass ratio of red mud to phosphogypsum in the modified composite material is 7:3, its performance is most outstanding: the pH value remains stable at 8.03, the electrical conductivity (EC) is maintained at an appropriate level of 4.89 mS/cm, and the concentrations of phosphate (PO_4^{3-}) and fluoride ions (F^-) are reduced to 0.36 mg/L and 1.34 mg/L, respectively. This successfully achieves the transformation from industrial Class II slag to Class I slag.

(2) After modification, the composite material exhibits a high specific surface area, moderate pore size, and maximized pore volume, significantly enhancing its adsorption performance. The iron salt treatment not only introduces iron-based compounds and alters the mineral phase structure of the original mixed material, but also achieves the solidification and stabilization of characteristic pollutants, forming a compact and stable structure.

(3) In the composite material, synergistic interlocking effects and calcium supplementation–alkali reduction mechanisms work together. The strong alkaline conditions of red mud activate the silicon-aluminum components on the surface of phosphogypsum, promoting the formation of C-S-H gel. Simultaneously, under the combined action of $Fe(OH)_3$ and $Al(OH)_3$, the composite material effectively adsorbs, encapsulates, and co-precipitates toxic pollutants. Additionally, the appropriate alkalinity of the composite material enhances its electrostatic attraction to negatively charged ions such as F^-, HPO_4^{2-}, and PO_4^{3-}. The gel structure and the excellent specific surface area and interlayered structure of AFt provide abundant active sites for the adsorption and stabilization of heavy metals, immobilizing them within the crystal structure. As a result, the toxic leaching content of the modified composite material fully complies with the standard requirements for Class I solid waste.

(4) Despite the promising results, this study has certain limitations that provide opportunities for future research. First, the experiments were conducted on a laboratory scale, and the long-term performance of the composite material in field conditions needs further validation. Second, only ryegrass was used in the pot experiments; future studies should include a wider range of plant species to assess the general applicability of the composite material. Third, the complex interactions between the composite material and environmental factors (e.g., climate change, soil microbial activity) were not considered, which should be addressed in future research. Finally, a detailed techno-economic analysis is required to evaluate the feasibility of large-scale production and application of the composite material. These limitations highlight the need for further research to fully realize the potential of red mud–phosphogypsum composites in ecological restoration and environmental management.

Author Contributions: B.L.: Conceptualization, methodology, formal analysis, data curation, visualization, writing—original draft. F.L.: validation, data curation, writing—review and editing. J.Z.: Sampling, Supervision, Project administration, Resources. Z.C.: Supervision, Project administration. All authors have read and agreed to the published version of the manuscript.

Funding: This work was supported by the Provincial Natural Science Foundation of Guizhou, China (Qiankehejichu-ZK-[2022] Zhongdian014), and the Natural Science Foundation of Guiyang, China (Zhukehetong-[2024]-1-13).

Data Availability Statement: All datasets used during the current study are available from the corresponding author on reasonable request.

Acknowledgments: We than Guizhou University's College of Resources and Environmental Science for providing access to their laboratories and instruments.

Conflicts of Interest: The authors declare no conflicts of interest.

References

1. Hua, Y.; Heal, K.V.; Friesl-Hanl, W. The use of red mud as an immobiliser for metal/metalloid-contaminated soil: A review. *J. Hazard. Mater.* **2017**, *325*, 17–30. [PubMed]
2. Yang, J.; Dong, S.; Ma, L.; Dai, Q.; Zheng, D.; Huang, B.; Sun, M.; Hu, B.; Du, W.; Xie, L.; et al. Review on high-value utilization of phosphogypsum: Utilization of calcium and oxygen resources present in phosphogypusm. *Sep. Purif. Technol.* **2024**, *344*, 127246.
3. Xue, S.; Zhu, F.; Kong, X.; Wu, C.; Huang, L.; Huang, N.; Hartley, W. A review of the characterization and revegetation of bauxite residues (Red mud). *Environ. Sci. Pollut. Res.* **2016**, *23*, 1120–1132.
4. Du, P.; Wang, P.; Zhang, X.; Wen, G.; Wang, Y. Properties, hazards and valuable metal recovery technologies of red mud: A review. *Particuology* **2024**, *93*, 328–348.
5. Hao, H.; Liu, X.; Dong, X.; Liu, Y.; Li, J.; Li, J.; Xu, X.; Chang, S. Study on the solidification/stabilization of Cu(II) and Cd(II)-contaminated soil by fly ash-red mud based geopolymer. *Constr. Build. Mater.* **2025**, *469*, 140515.
6. Liu, Y.; Chen, Q.; Dalconi, M.C.; Molinari, S.; Valentini, L.; Wang, Y.; Sun, S.; Wang, P.; Artioli, G. Retention of phosphorus and fluorine in phosphogypsum for cemented paste backfill: Experimental and numerical simulation studies. *Environ. Res.* **2022**, *214*, 113775.
7. Shi, Y.; Ma, Y.; Min, J.; He, J.; Li, Y.; Lu, X.; Wang, H. Cemented phosphogypsum backfill utilizing microbial induced carbonate precipitation without additional calcium source. *Constr. Build. Mater.* **2025**, *460*, 139586.
8. Liu, Z.; Guo, R.; Fu, C.; Liao, S.; Li, X.; Wang, X.; Lin, R.-S. Microwave activated red mud-based geopolymer: Synergistic solid waste utilization and heavy metal immobilization mechanism. *Constr. Build. Mater.* **2025**, *470*, 140564.
9. Wang, C.-Q.; Chen, S.; Huang, D.-M.; Huang, Q.-C.; Li, X.-Q.; Shui, Z.-H. Safe environmentally friendly reuse of red mud modified phosphogypsum composite cementitious material. *Constr. Build. Mater.* **2023**, *368*, 130348.
10. Gao, Y.; Li, Z.; Zhang, C.; Zhang, J. Study on occurrence form and solidification mechanism of alkaline components in red mud. *J. Mater. Cycles Waste Manag.* **2023**, *25*, 3758–3775.
11. Xue, H.; Lv, G.; Zhang, T.-A. Progress of Solid Waste Red Mud in the Field of Ecology and Environment. *Water Air Soil Pollut.* **2025**, *236*, 176. [CrossRef]
12. Dong, W.; Deng, X.; Chai, L.; Zhang, Y.; Chen, H.; Wu, H.; Chi, R. Leaching Characteristics and Mechanisms of Fluorine and Phosphorus from Phosphogypsum. *Molecules* **2025**, *30*, 5. [CrossRef] [PubMed]
13. Liu, Y.; Zhang, L.; Xue, B.; Chen, L.; Wang, G.; Wang, J.; Wan, H.; Lin, X.; Zhu, G. Simulation of red mud/phosphogypsum-based artificial soil engineering applications in vegetation restoration and ecological reconstruction. *Sci. Total Environ.* **2024**, *951*, 175656. [CrossRef]
14. Chen, T.; Wang, L.; He, B.; Peng, X.; Nie, X.; Ma, F.; Han, P.; Bai, X. Study on the solidification/stabilization of cadmium-contaminated soil by red mud-assisted blast furnace slag under excitation conditions. *J. Clean. Prod.* **2024**, *435*, 140505. [CrossRef]
15. Habibi, H.; Mokmeli, M.; Shakibania, S.; Pirouzan, D.; Pourkarimi, Z. Separation and recovery of titanium and scandium from the red mud. *Sep. Purif. Technol.* **2023**, *317*, 123882. [CrossRef]
16. He, D.; Xiong, Y.; Wang, L.; Sun, W.; Liu, R.; Yue, T. Arsenic (III) Removal from a High-Concentration Arsenic (III) Solution by Forming Ferric Arsenite on Red Mud Surface. *Minerals* **2020**, *10*, 583. [CrossRef]
17. Xu, X.; Cheng, G.; Xu, M. Effects of bio-organic fertilizer and sticktights on the ecological restoration of bauxite residue and dehydrated mineral slime loam disposal. *Chin. J. Environ. Eng.* **2023**, *17*, 958–966.
18. Han, Y. Research on the Preparation and Application of Red Mud Adsorbent Materials. Master's Thesis, Beijing University of Chemical Technology, Beijing, China, 2004.
19. Ji, X.; Dai, C.; Cui, Z.; Zhou, R. Research on Engineering Characteristics of Curing Agent Stabilized Phosphogypsum Roadbed Filler. *China J. Highw. Transp.* **2021**, *34*, 225–233.
20. Zemni, S.; Hajji, M.; Triki, M.; M'Nif, A.; Hamzaoui, A.H. Study of phosphogypsum transformation into calcium silicate and sodium sulfate and their physicochemical characterization. *J. Clean. Prod.* **2018**, *198*, 874–881. [CrossRef]
21. Liu, Y.; Yang, Z.; Zhang, L.; Wan, H.; Deng, F.; Zhao, Z.; Wang, J. Characteristics of Bacterial Community Structure and Function in Artificial Soil Prepared Using Red Mud and Phosphogypsum. *Microorganisms* **2024**, *12*, 1886. [CrossRef]
22. Li, W.; Wang, J.; Xu, R.; Du, S.; Qiao, Y.; Chen, H. Effects of Sludge Biochar Addition on Ryegrass and Soil Nutrient Properties. *Acta Agrestia Sin.* **2024**, *32*, 1295–1302.
23. Dong, C.; Zhou, X.; Ma, R.; Liu, N.; Ji, S.; Liu, Y. Study on the production of soilless turf with high humidity bamboo shavings instead of commercial peat. *Grassl. Turf* **2024**, *44*, 49–56.

24. *HJ GB8978-1996*; Integrated Wastewater Discharge Standard. Institute of Environmental Standards, Ministry of Ecology and Environment of the People's Republic of China: Beijing, China, 1996.
25. Liu, Y.; Liu, F.; Yang, A.; Li, Q.; Huang, H. Removal effect of modified red mud on nitrogen, phosphorus and dissolved organic matter in livestock wastewater. *Saf. Environ. J.* **2013**, *13*, 13–16.
26. Zeng, W.; Yi, H.; Liu, F.; Zhu, J.; He, Y.; Zhai, N.; An, N.; Zhao, J. Effect of Modified Phosphogypsum on the Growth of Ryegrass and Leachate Filtration. *Non-Met. Mines* **2023**, *46*, 28–32.
27. Xing, Y.; Zhou, K.; Zhang, X.; Lei, Q.; Peng, C.; Shi, Y.; Chen, W. Application of recycled ferric chloride for alkalinity regulation of bauxite residue. *J. Clean. Prod.* **2021**, *305*, 127174.
28. *HJ 557-2010*; Solid Waste—Extraction Procedure for Leaching Toxicity—Horizontal Vibration Method. China Environmental Science Press: Beijing, China, 2010.
29. *GB 11893-1989*; Water Quality-Determination of Total Phosphorus-Ammonium Molybdate Spectrophotometric Method. Ministry of Ecology and Environment of the People's Republic of China: Beijing, China, 1990.
30. *GB 7484-1987*; Water Quality-Determination of Fluoride-Ion Selective Electrode Method. Ministry of Ecology and Environment of the People's Republic of China: Beijing, China, 1987.
31. Liang, J.; Zhang, S.; Huang, J.; Huang, S.; Zheng, L.; Sun, S.; Zhong, Z.; Zhang, X.; Yu, X. Comprehensive insights into the inorganic coagulants on sludge dewatering: Comparing aluminium and iron salts. *J. Chem. Technol. Biotechnol.* **2019**, *94*, 1534–1550.
32. Guo, B.; Zhang, S.; Xu, X.; Gao, B.; Li, Q.; Yue, Q. An enhanced coagulation using ferric chloride and poly-ferric chloride coagulant assisted by polyamidine: Performance and mechanisms. *Chin. Chem. Lett.* **2023**, *34*, 108379.
33. Xue, S.; Li, M.; Jiang, J.; Millar, G.J.; Li, C.; Kong, X. Phosphogypsum stabilization of bauxite residue: Conversion of its alkaline characteristics. *J. Environ. Sci.* **2019**, *77*, 1–10.
34. Courtney, R.; Kirwan, L. Gypsum amendment of alkaline bauxite residue—Plant available aluminium and implications for grassland restoration. *Ecol. Eng.* **2012**, *42*, 279–282.
35. Zhao, B.; Wang, Y.; Ma, L.; Li, Y.; Deng, Y.; Chen, X.; Xu, Z. Adding an appropriate proportion of phosphogypsum ensured rice husk and urea composting to promote the compost as substrate utilization. *Bioresour. Technol.* **2022**, *344*, 126301.
36. Di Carlo, E.; Boullemant, A.; Courtney, R. Ecotoxicological risk assessment of revegetated bauxite residue: Implications for future rehabilitation programmes. *Sci. Total Environ.* **2020**, *698*, 134344.
37. Das, D.; Rout, P.K. A Review of Coal Fly Ash Utilization to Save the Environment. *Water Air Soil Pollut.* **2023**, *234*, 128.
38. Zhu, S.; Zhu, D.; Wang, X. Removal of fluorine from red mud (bauxite residue) by electrokinetics. *Electrochim. Acta* **2017**, *242*, 300–306.
39. Cao, W.; Yi, W.; Peng, J.; Li, G.; Yin, S. Preparation of anhydrite from phosphogypsum: Influence of phosphorus and fluorine impurities on the performances. *Constr. Build. Mater.* **2022**, *318*, 126021.
40. Wang, M.; Liu, X. Applications of red mud as an environmental remediation material: A review. *J. Hazard. Mater.* **2021**, *408*, 124420. [PubMed]
41. Shen, Z.; Li, J.; Li, C.; Liao, Z.; Mei, N.; Luo, C.; Wang, D.; Zhang, C. Source apportionment of heavy metals in farmland soil surrounding red mud stockpiles based on APCS-MLR and PMF models. *Environ. Sci.* **2024**, *45*, 1058–1068.
42. Li, B.; Li, C.; You, C.; Li, J. Distribution characteristics and risk assessment of major pollutants in water environment around phosphogypsum stockpile area. *Chem. Environ. Prot.* **2024**, *44*, 279–285.
43. Ma, F.; Chen, L.; Lin, Z.; Liu, Z.; Zhang, W.; Guo, R. Microstructure and Key Properties of Phosphogypsum-Red Mud-Slag Composite Cementitious Materials. *Materials* **2022**, *15*, 6096. [CrossRef]
44. Ge, J.; Xiao, Y.; Kuang, J.; Liu, X. Research progress of chlorination roasting of heavy metals in solid waste. *Surf. Interfaces* **2022**, *29*, 101744.
45. Liu, Y.; Zhang, L.; Chen, L.; Xue, B.; Wang, G.; Zhu, G.; Gou, W.; Yang, D. Potential of artificial soil preparation for vegetation restoration using red mud and phosphogypsum. *Sci. Total Environ.* **2024**, *941*, 173553.
46. Yuan, J.; Li, Y.; Chen, S.; Li, D.; Tang, H.; Chadwick, D.; Li, S.; Li, W.; Li, G. Effects of phosphogypsum, superphosphate, and dicyandiamide on gaseous emission and compost quality during sewage sludge composting. *Bioresour. Technol.* **2018**, *270*, 368–376. [CrossRef]
47. Li, X.; Xie, Y.; Jiang, F.; Wang, B.; Hu, Q.; Tang, Y.; Luo, T.; Wu, T. Enhanced phosphate removal from aqueous solution using resourceable nano-CaO_2/BC composite: Behaviors and mechanisms. *Sci. Total Environ.* **2020**, *709*, 136123. [CrossRef] [PubMed]
48. Li, J.; Li, B.; Huang, H.; Lv, X.; Zhao, N.; Guo, G.; Zhang, D. Removal of phosphate from aqueous solution by dolomite-modified biochar derived from urban dewatered sewage sludge. *Sci. Total Environ.* **2019**, *687*, 460–469. [CrossRef]
49. Xie, Y.; Huang, J.; Wang, H.; Lv, S.; Jiang, F.; Pan, Z.; Liu, J. Simultaneous and efficient removal of fluoride and phosphate in phosphogypsum leachate by acid-modified sulfoaluminate cement. *Chemosphere* **2022**, *305*, 135422. [CrossRef] [PubMed]
50. Kim, M.; Choong, C.E.; Hyun, S.; Park, C.M.; Lee, G. Mechanism of simultaneous removal of aluminum and fluoride from aqueous solution by La/Mg/Si-activated carbon. *Chemosphere* **2020**, *253*, 126580. [CrossRef] [PubMed]

51. Rashid, U.S.; Das, T.K.; Sakthivel, T.S.; Seal, S.; Bezbaruah, A.N. GO-CeO_2 nanohybrid for ultra-rapid fluoride removal from drinking water. *Sci. Total Environ.* **2021**, *793*, 148547. [CrossRef]
52. Matinfar, M.; Nychka, J.A. A review of sodium silicate solutions: Structure, gelation, and syneresis. *Adv. Colloid Interface Sci.* **2023**, *322*, 103036. [CrossRef]
53. Getman-Pickering, Z.L.; Stack, G.M.; Thaler, J.S. Fertilizer quantity and type alter mycorrhizae-conferred growth and resistance to herbivores. *J. Appl. Ecol.* **2021**, *58*, 931–940. [CrossRef]
54. Pedersen, I.F.; Eriksen, J.; Christensen, B.T.; Rubæk, G.H. The Jyndevad Experiment: Revealing long-term interactions between liming and phosphorus fertilization in a coarse sand soil. *Eur. J. Agron.* **2025**, *162*, 127392. [CrossRef]
55. Meng, D.; Li, S.; Li, Z.; Chen, W.; Li, Z.; Zhou, J.; Guo, Y.; Li, H. Possibility of using industrial by-product combinations to remediate cadmium and arsenic contaminated soil. *Appl. Soil Ecol.* **2024**, *203*, 105654. [CrossRef]
56. Wang, L.; Chen, L.; Tsang, D.C.; Zhou, Y.; Rinklebe, J.; Song, H.; Kwon, E.E.; Baek, K.; Ok, Y.S. Mechanistic insights into red mud, blast furnace slag, or metakaolin-assisted stabilization/solidification of arsenic-contaminated sediment. *Environ. Int.* **2019**, *133*, 105247. [PubMed]
57. Wang, J.; Cao, H.; Qi, X.; Zhi, G.; Wang, J.; Huang, P. Preparation of nano red mud gels using red mud for the encapsulation and stabilization of arsenic in arsenic-bearing gypsum sludge. *Sep. Purif. Technol.* **2024**, *341*, 126680. [CrossRef]
58. Feng, Y.-S.; Zhou, S.-J.; Zhou, A.; Jiang, N.-J.; Xia, W.-Y.; Wang, S.; Du, Y.-J. Environmental performance of reusing a contaminated soil solidified/stabilized by a low-carbon binder as roadway subgrade material. *J. Clean. Prod.* **2022**, *375*, 134125. [CrossRef]
59. Kiventerä, J.; Piekkari, K.; Isteri, V.; Ohenoja, K.; Tanskanen, P.; Illikainen, M. Solidification/stabilization of gold mine tailings using calcium sulfoaluminate-belite cement. *J. Clean. Prod.* **2019**, *239*, 118008. [CrossRef]
60. Zhang, J.; Yang, F.; Yao, X.; Cao, H.; Duan, W.; Dong, X. The synergistic action mechanisms of ternary industrial waste stabilized lead ion contaminated soil. *Constr. Build. Mater.* **2023**, *409*, 133827.
61. Liu, S.; Liu, Z.; Zhu, H.; Wang, Z.; Guo, J.; Zhang, X.; Yu, H.; Yue, X.; Ning, P.; Li, B. The roles of red mud as desulfurization and denitrification in flue gas: A review. *J. Environ. Chem. Eng.* **2023**, *11*, 109770.
62. Wu, Y.; Li, M.; Zhu, F.; Hartley, W.; Liao, J.; An, W.; Xue, S.; Jiang, J. Variation on leaching behavior of caustic compounds in bauxite residue during dealkalization process. *J. Environ. Sci.* **2020**, *92*, 141–150. [CrossRef] [PubMed]
63. Xiao, J.; Zhang, J.; Zhang, H.; Bi, Y.; Yue, H.; Xu, R. Preparation and characterization of organic red mud and its application in asphalt modification. *Constr. Build. Mater.* **2023**, *367*, 130269.
64. Yu, J.; Ji, F.; Lv, Q.; Li, W.; Lin, Z.; Peng, Y. Mechanical property and microstructure of fly ash-based geopolymer by calcium activators. *Case Stud. Constr. Mater.* **2024**, *21*, e03811.
65. Li, H.; Li, H.; Du, M.; Zhou, E.; Leow, W.R.; Liu, M. A perspective on field-effect in energy and environmental catalysis. *Chem. Sci.* **2025**, *16*, 1506–1527.
66. Wu, H.; He, M.; Cheng, J.; Wang, T.; Che, Y.; Du, Y. Study on the synergistic effects of OPC and silica fume on the mechanical and microstructural properties of geopolymer mortar. *Constr. Build. Mater.* **2024**, *434*, 136740.
67. Wang, Y.; Liu, P.; Kong, D.; Li, Y.; Fu, X.; Ren, C.; Chen, M. Investigation of the properties and microscopic mechanism of red mud-phosphogypsum-based composite cementitious materials. *J. Build. Eng.* **2025**, *101*, 111962.

Disclaimer/Publisher's Note: The statements, opinions and data contained in all publications are solely those of the individual author(s) and contributor(s) and not of MDPI and/or the editor(s). MDPI and/or the editor(s) disclaim responsibility for any injury to people or property resulting from any ideas, methods, instructions or products referred to in the content.